ELSEVIER

Journal of Photochemistry and Photobiology A: Chemistry 113 (1998) 233–241

Journal of Photochemistry and Photobiology A:Chemistry

Electron transfer photosensitized by a tin lipoporphyrin in solution, micelles, and at water–organic solvent interfaces

Xing-Zhi Song [a,b], Song-Ling Jia [a,b], Michiko Miura [c], Jian-Guo Ma [a,b], John A. Shelnutt [a,b,*]

[a] *Materials Theory and Computation Department, Sandia[1] National Laboratories, Albuquerque, NM 87185-1349, USA*

[b] *Department of Chemistry, University of New Mexico, Albuquerque, NM 87131, USA*

[c] *Medical Department, Brookhaven National Laboratory, Upton, NY 11973, USA*

Received 2 June 1997; received in revised form 16 October 1997

Abstract

Electron transfer photosensitized by a tin lipoporphyrin [Sn(IV) octakis((methoxycarbonyl)-methyl)-*meso*-tetrakis-(((eicosanyloxy)carbonyl)phenyl)-porphyrin (SnLipoP)] is investigated under various solution conditions using a donor–SnLipoP–methylviologen (MV^{2+}) ternary system, where the donor is triethanolamine (TEA) or ethylenediaminetetraacetic acid (EDTA). The photoreaction of SnLipoP is compared with the photoreactions sensitized by common Sn porphyrins like tin protoporphyrin IX (SnPP) and octaethylporphyrin (SnOEP). A constant photoreaction rate is observed in a water/organic solvent (hexane, benzene) two-phase system in which the porphyrin (SnLipoP, SnOEP) is in the organic solvent and MV^{2+} is in the aqueous phase. The rate is monitored by the change in the UV–visible absorption spectra produced by aqueous methylviologen radical $MV^{\bullet+}$. In contrast with the two-phase system, macroscopically homogeneous solutions (aqueous SnPP and micellar solutions of SnLipoP, SnPP and SnOEP) give pseudo-logarithmic rates. These electron-transfer processes are completely consistent with reductive primary electron transfer to the tin porphyrin and optical shielding effects. Differences in the rates for SnLipoP and the other Sn porphyrins are explained by structural differences in the porphyrins. In particular, the structure of the porphyrin influences the phase in which the porphyrin resides, its location relative to interfacial regions, and the way it interacts with itself and other system components.

Keywords: Electron transfer; Tin lipoporphyrin; Triethanolamine; Ethylenediaminetetraacetic acid

1. Introduction

There is a lasting interest in photoinduced redox reactions of three-component systems that contain a photosensitizer, an electron donor, and an electron acceptor [1–18], especially those in which a metalloporphyrin acts as the photosensitizer. Depending on the redox potential of the excited metalloporphyrin, the primary process in the ternary system can be oxidative (e.g., zinc porphyrins [15,18]) or reductive (e.g., tin porphyrins [13,14,16,19]). These ternary systems have been extensively studied in aqueous solution [13,20] and organized media, such as micelles [21–25], vesicles [18,26,27], and microemulsions [10,28–33]. In some cases, they provide useful models of biological transmembrane electron transfer, and they are interesting from the standpoint of solar energy conversion and storage.

Here, we investigate ternary photoredox systems for a new type of photosensitizing metalloporphyrin, one that can be incorporated into organized supramolecular assemblies such as membranes, micellar systems, and thin films [34]. Using molecular simulations, we designed and subsequently synthesized a lipoporphyrin with a polar porphyrin head group and four nonpolar tails [35]. The structure of the tin derivative of the lipoporphyrin, octakis((methoxycarbonyl)-methyl)-*meso*-tetrakis(((eicosanyloxy)-carbonyl)-phenyl)-porphyrin (LipoP), is shown in Fig. 1a. SnLipoP has the following desired properties: (1) solvent accessibility of the porphyrin head groups at the surface of aqueous micelles and Langmuir–Blodgett (LB) films, (2) the lack of aggregation of individual lipoporphyrin molecules, and (3) photochemical activity. The first two of these properties were examined in previous works [35,36]. Here, we report the photochemical properties of the tin derivative of LipoP. It is expected that SnLipoP will have altered photochemical behavior compared with common Sn porphyrins. This is partly because of its unique structure in which the porphyrin

* Corresponding author.

[1] Sandia is a multiprogram laboratory operated by Sandia, a Lockheed Martin, for the United States Department of Energy under Contract DE-AC04-94AL85000.

1010-6030/98/$19.00
PII S1010-6030(97)00322-5

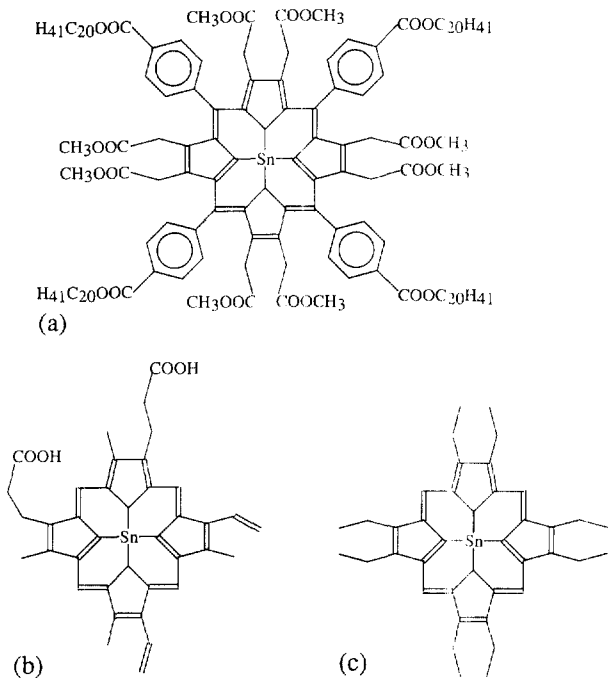

Fig. 1. Molecular structures of tin octakis((methoxycarbonyl)-methyl)-*meso*-tetrakis((eicosanyloxy)carbonyl)phenyl)-porphyrin, SnLipoP (a), tin protoporphyrin, SnPP (b), and tin octaethylporphyrin, SnOEP (c).

moiety provides the polar head of the lipid, and partly because of the strong nonplanar distortion of the porphyrin [37].

Photoreaction rates for production of reduced methylviologen are measured for SnLipoP in micelles and in a water/hexane two-phase system. For comparison under the same conditions, electron-transfer reactions photosensitized by two other porphyrins (shown in Fig. 1) are also studied in water, micelles, and in the water/organic solvent two-phase system. Tin protoporphyrin IX (SnPP) is water-soluble, and tin octaethylporphyrin (SnOEP) is water-insoluble. Thus, the two porphyrins reside within different phases in the two-phase system and at different locations in the micelles. The effect of surfactant charge on the electron-transfer process is also investigated by using cationic and anionic surfactants, cetyltrimethylammonium bromide (CTAB) and sodium dodecyl sulfate (SDS), respectively. Methylviologen (MV^{2+}) is the electron acceptor, providing a blue color in its reduced form ($MV^{\bullet+}$) that is easily monitored by UV–visible absorption spectroscopy. Ethylenediaminetetraacetic acid (EDTA) and triethanolamine (TEA) are charged and neutral, respectively. The solubilities of these donors in water, benzene, and hexane are well known, allowing their respective locations in various phases of the photochemical systems to be predicted. The differences in photoreactivity of the porphyrins can be explained in terms of the differences in porphyrin structure, optical-shielding effects, the distributions of the porphyrin and other components among the phases, and the effects of surfactant charge.

2. Experimental details

2.1. Materials

The synthesis of SnLipoP was described previously [35]. SnPP and SnOEP were purchased from Porphyrin Products, Methylviologen (MV^{2+}), SDS, TEA, CTAB, and the tetrasodium salt of EDTA were purchased from Aldrich and used without further purification.

2.2. Photoreaction rate measurements and UV–visible absorption spectroscopy

All the solutions for photoreaction were prepared in low light and kept in the dark before reaction. The photoreaction solutions for donor–porphyrin–acceptor ternary systems in micelles were prepared by adding known amounts of each component into water and sonicating for several minutes until a clear solution was obtained. The photoreaction solutions for donor–SnPP–MV^{2+} system in water were prepared by adding weighed amounts of methylviologen and EDTA (or TEA) to a pre-prepared SnPP aqueous solution at pH 12. The water/organic solvent two-phase reaction system consisted of separated organic solvent and water solutions with the aqueous phase at the bottom of the cell. Hexane and benzene are used as the organic solvent for SnLipoP and SnOEP, respectively. The photoreaction was driven by irradiation with white light from a 25-W tungsten (Tensor) lamp from one direction of a covered four-window absorption cell. The photoreaction was monitored in the direction perpendicular to irradiation as illustrated in Fig. 2a and b using a HP8452A diode array spectrophotometer (Hewlett-Packard). Upon irradiation of the ternary system, $MV^{\bullet+}$ is rapidly built up in the aqueous phase. UV–visible absorption spectra of the aqueous phase were taken at 15-s intervals at the beginning of reaction, and at longer intervals at later times. The concentration of $MV^{\bullet+}$ was calculated from the maximum absorbance at 602 nm ($\varepsilon_{602} = 1.0 \cdot 10^4\ M^{-1}\ cm^{-1}$) [13]. The initial reaction rate was obtained from the [$MV^{\bullet+}$]–time slope obtained from the linear least-squares fit of the first five experimental points taken within the first 1.5 min.

The behavior of SnPP in aqueous solution and micelles (CTAB and SDS) from pH 1 to 13 was studied by UV–visible absorption spectroscopy. The SnPP solution was titrated starting at high pH with concentrated HCl.

2.3. Molecular mechanics

Molecular energy-optimization calculations are performed using Polygraf software (Molecular Simulations) and a hybrid force field based on the Dreiding force field [38]. Briefly, the Dreiding force field was modified to include atom types specific to the porphyrin macrocycle [39]. Force constants for the atom types of the macrocycle were obtained from normal coordinate analysis of nickel porphyrins [40–43]. Equilibrium bond distances, bond angles, torsions, and

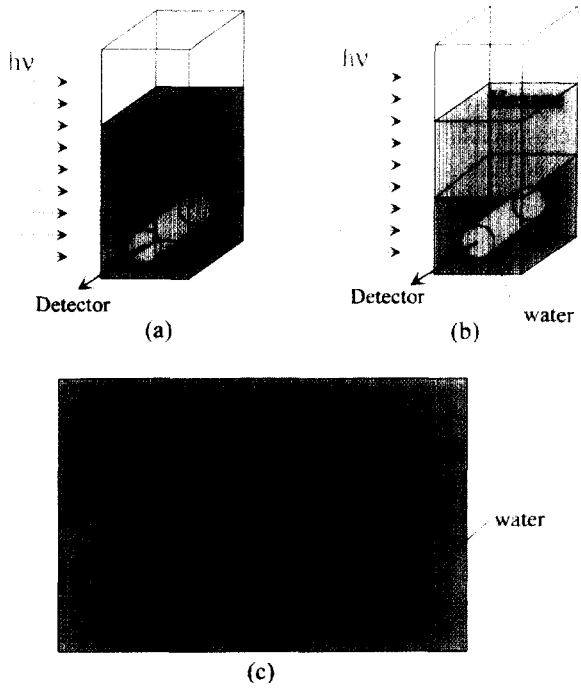

Fig. 2. Illustrations of the irradiation and detection of the photoreaction in a macroscopically homogeneous solution (water and micelles) (a) in at two-phase hexane/water system (b), and the photoreaction mechanism in a macroscopically homogeneous solution (c).

inversions were optimized to reproduce the crystal structure of the triclinic B form of NiOEP [44]. The force field has been shown to accurately predict the crystal structures of both planar and nonplanar metalloporphyrins [45–50], especially after recent improvements [51].

3. Results and discussion

3.1. Kinetic analysis

Methylviologen cation radical, $MV^{\bullet+}$, the product of the photoreaction, is stable under our experimental conditions. Fig. 3 shows the change in the UV–visible absorption spectrum of the aqueous phase during photoreduction of $MV^{\bullet+}$ sensitized by SnLipoP in the water/hexane two-phase system with TEA as the donor. The two-phase photoreaction is illustrated in Fig. 2b. For this two-phase system, a linear relationship between the $MV^{\bullet+}$ concentration and irradiation time is observed as shown in the inset of Fig. 3. In contrast, for macroscopically homogeneous (micellar and aqueous) solutions in which the reactants, photosensitizer, and products are in the same phase, a pseudo-logarithmic relationship between $[MV^{\bullet+}]$ and irradiation time is observed. Fig. 4 shows this relationship for the EDTA–SnPP–MV^{2+} system in aqueous solution at pH 12.

A well-known photoreaction mechanism based on a reductive primary electron-transfer process quantitatively explains the observed kinetics [52]. Because the redox potential of tin porphyrins in the triplet excited state (SnP^{*}/SnP^{-}, $+1.11$ v) is higher than that of the electron donors ($EDTA^{+}$/EDTA, TEA^{+}/TEA, $+0.82$ v) [11,14,53–55], the excited tin porphyrin accepts an electron from the donor. In addition, the redox potential of the tin-porphyrin anion (SnP/SnP^{-}, -0.66 V) is lower than that of methylviologen (MV^{2+}/MV^{+}, -0.45 v); thus, SnP^{-} reduces methylviologen. The net result of these photoinduced reactions is the transport of

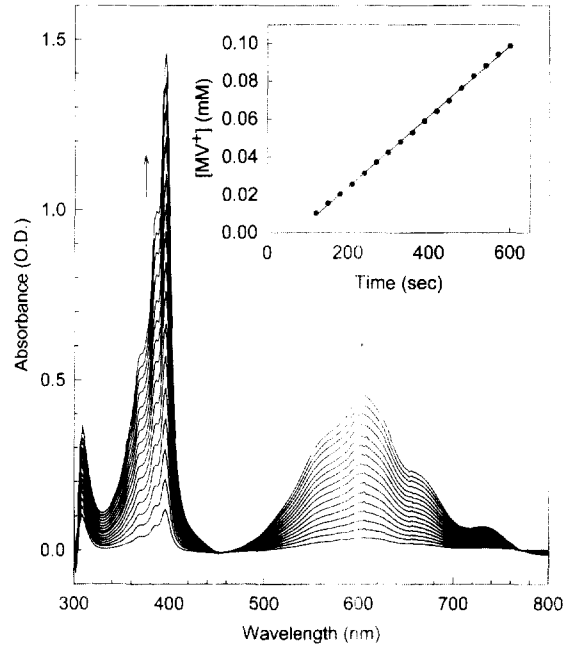

Fig. 3. UV–visible absorption spectra taken in the water phase at different times showing the photoreduction of methylviologen ($[MV^{2+}] = 0.020$ M) to $MV^{\bullet+}$ by triethanolamine ([TEA] = 0.40 M) sensitized by SnLipoP ([SnLipoP] = $\sim 10^{-6}$ M in hexane) for the two-phase hexane/water system. The insert shows the linear dependence of $MV^{\bullet+}$ concentration on irradiation time.

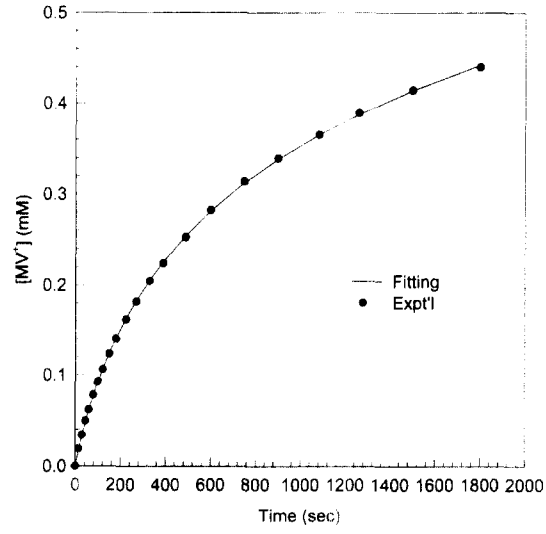

Fig. 4. The dependence of $MV^{\bullet+}$ concentration on irradiation time (circles) for photo-reduction of methylviologen ($[MV^{2+}] = 5$ mM) by EDTA ([EDTA] = 0.2 M) sensitized by SnPP ([SnPP] = 5.86 μM) in water (pH = 12), and the curve-fitting results (squares) with equation $[MV^{\bullet+}] = a\ln(1 + bt)$.

an electron from the donor to methylviologen as illustrated in Fig. 2c. The complete reaction scheme is given in Eqs. (1)–(6). This mechanism takes into consideration the absorption of light by methylviologen cation radical and the deactivation of porphyrin and methylviologen–cation–radical excited states.

$$P + h\nu \xrightarrow{k_1} P^* \quad (1)$$

$$P^* + EDTA \xrightarrow{k_2} P^{\bullet -} + EDTA^{\bullet +} \quad (2)$$

$$P^{\bullet -} + MV^{2+} \xrightarrow{k_3} P + MV^{\bullet +} \quad (3)$$

$$P^* + S \xrightarrow{k_4} P + S \quad (4)$$

$$MV^{\bullet +} + h\nu \xrightarrow{k_5} MV^{\bullet +*} \quad (5)$$

$$MV^{\bullet +*} + S \xrightarrow{k_6} MV^{\bullet +} + S \quad (6)$$

With this reaction scheme, at steady state the rate for $MV^{\bullet +}$ production is,

$$\frac{d[MV^{\bullet +}]}{dt} = K[P]I_{total}, \quad (7)$$

since the solvent concentration is constant, as is the electron–donor concentration, which is in great excess. In Eq. (7), the constant

$$K = \frac{k_1 k_2 [EDTA]}{k_2[EDTA] + k_4[S]}$$

In the two-phase reaction, the light intensity I_{total} absorbed by the photosensitizer molecules is constant, and since the porphyrin concentration is also constant, integration of Eq. (7) gives,

$$[MV^{\bullet +}] = K[P]I_{total}t. \quad (8)$$

Thus, the $MV^{\bullet +}$ concentration increases linearly with irradiation time as shown in Fig. 3.

For the macroscopically homogeneous solutions, however, the light intensity I seen by porphyrin molecules at l cm depends on the absorption of light by both the porphyrin and the methylviologen cation radical, since they occupy the same phase. This produces a *shielding* effect of $MV^{\bullet +}$ on the absorption of light by the porphyrin. Specifically, the light intensity after passing a depth l cm is,

$$I = I_0 e^{-\varepsilon_P l[P]} e^{-\varepsilon_{MV^{\bullet +}} l[MV^{\bullet +}]} \quad (9)$$

If the photoreaction cell is thin, we can use the light intensity at the half width ($l = \frac{1}{2}L$) of the cell as the average intensity over the cell thickness L. In this case, after the integration of Eq. (7) we get,

$$[MV^{\bullet +}] = a \ln(1 + bt) \quad (10)$$

where $a = 1/\varepsilon_{MV^{\bullet +}} l$ and $b = \varepsilon_{MV^{\bullet +}} l K I_0 [P] e^{-\varepsilon_P l[P]}$. Thus, $[MV^{\bullet +}]$ has a pseudo-logarithmic dependence on irradiation time. Using Eq. (10) to fit the experimental data shown in Fig. 4, the fit to the data is almost exact. In summary, the mechanism quantitatively explains the different observed kinetic behaviors for photoreaction of the ternary systems in macroscopically homogeneous (micellar and aqueous) solutions and the water–organic solvent two-phase system.

When $t = 0$, the initial reaction rate is,

$$\left(\frac{d[MV^{\bullet +}]}{dt}\right)_0 = K I_0 [P] e^{-\varepsilon_P l[P]}. \quad (11)$$

Fig. 5 shows the dependence of initial photoreaction rate on porphyrin concentration for the EDTA–SnPP–MV^{2+} ternary system in aqueous solution at pH 12. Again, the kinetic treatment based on reactions (1) to (6) gives an almost exact fit to the experimental data using Eq. (11). (Further, the extinction coefficient of SnPP, ε_P, obtained from fitting [$1.48 \cdot 10^4$ $M^{-1} cm^{-1}$] is also in accordance with our experimental value [$1.58 \cdot 10^4$ $M^{-1} cm^{-1}$]).

3.2. Effect of porphyrin structure on photoreaction rates

The structural properties of the porphyrin determine its location in the reaction system, and this largely determines the photoreaction rates. Fig. 6 shows the structure of SnLipoP obtained from molecular mechanics calculations. This porphyrin consists of a hydrophilic porphyrin head group and four long hydrophobic alkyl tails. The carboxylic acid ester groups surrounding the porphyrin head group make it highly hydrophilic. When the porphyrin in hexane solution is added to a water surface, the porphyrin resides at the hexane/water interface [35]. The porphyrin head groups lie flat on the water phase, and the four hydrophobic tails are directed toward the hexane phase. Some SnLipoP is also dissolved in the bulk hexane phase, and there is likely to be constant dynamic exchange between the interfacial molecules and those in the

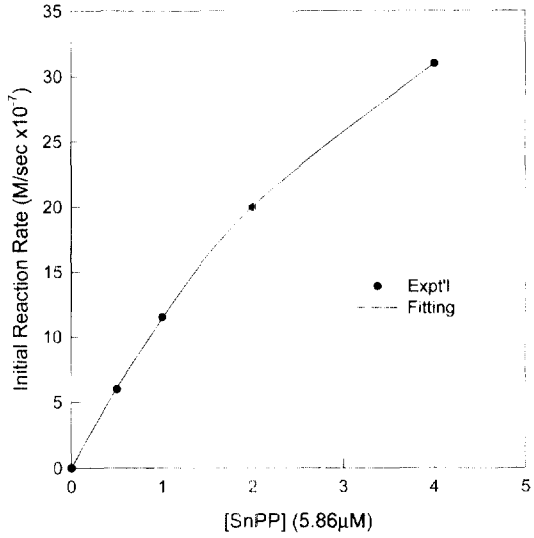

Fig. 5. The dependence of initial photoreaction rate on porphyrin (SnPP) concentration [P] (circles) in water (pH = 12, $[MV^{2+}] = 5$ mM, and [EDTA] = 0.2 M), and the curve-fitting results (squares) with equation $r_0 = a[P]e^{-\varepsilon_P l[P]}$.

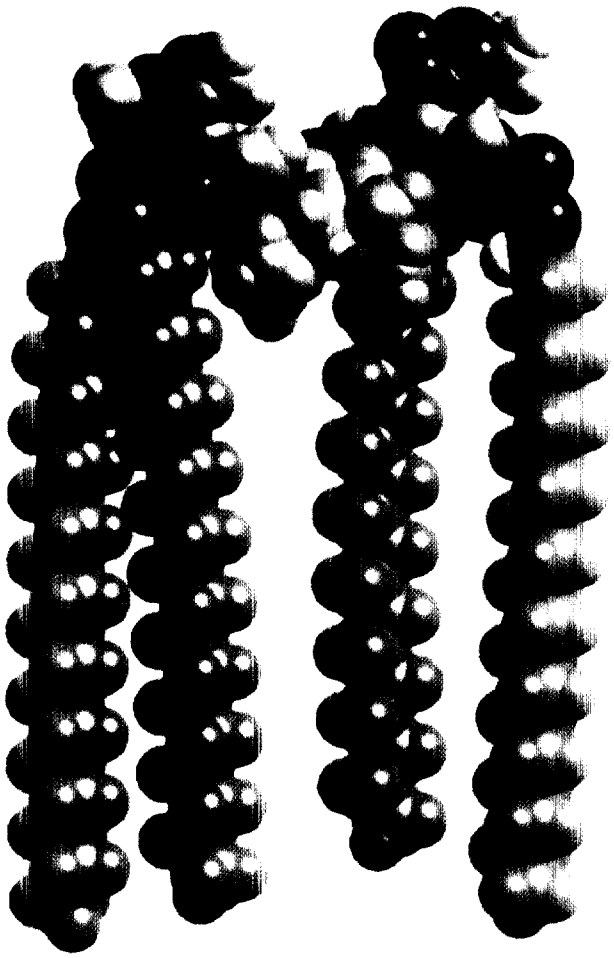

Fig. 6. The structure of SnLipoP calculated by molecular mechanics.

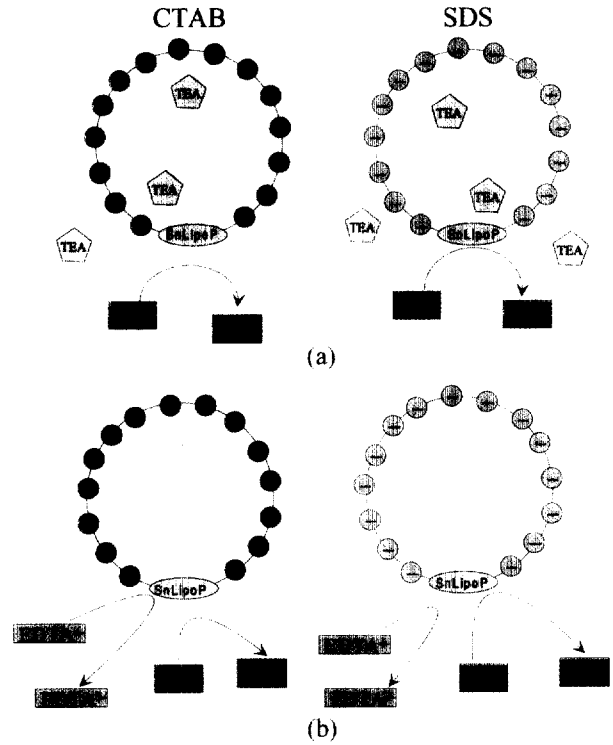

Fig. 7. The photoreactions sensitized by SnLipoP in CTAB (left panel) or in SDS (right panel) micelles with TEA (a) or with EDTA (b) as the electron donor.

organic solvent. When lipoporphyrin is dissolved in micelles, the porphyrin head groups will likely locate at the surface with the four tails inside the micelle, leaving one side of the macrocycle exposed to water as illustrated in Fig. 7.

Octaethylporphyrin and protoporphyrin have very different hydrophilicities. SnOEP is hydrophobic and can be dissolved in organic solvents, but not in water. When in aqueous micellar solutions, SnOEP will be located inside the hydrophobic interior of the micelle as illustrated in Fig. 8. SnPP is amphiphilic due to the hydrophilic carboxylate groups and the hydrophobic porphyrin macrocycle. When dissolved in a micellar solution, the hydrophobic macrocycle of SnPP will reside among the hydrophobic tails of micelles, with the two carboxylate groups at the surface of the micelles.

One large difference in the photoreaction rates of Table 1 is noted by comparing SnLipoP and SnOEP in the water/hexane two-phase systems. The molar rate for SnLipoP (0.24 s^{-1}) is significantly faster than for SnOEP (0.016 s^{-1}). For SnLipoP, its lipid properties help prolong the resident time of the porphyrin head group at the water–organic solvent interface. In fact, at any time, about 4% of the SnLipoP molecules occupy a monolayer at the interface. Thus, the lipid nature of SnLipoP provides an enhancement mechanism

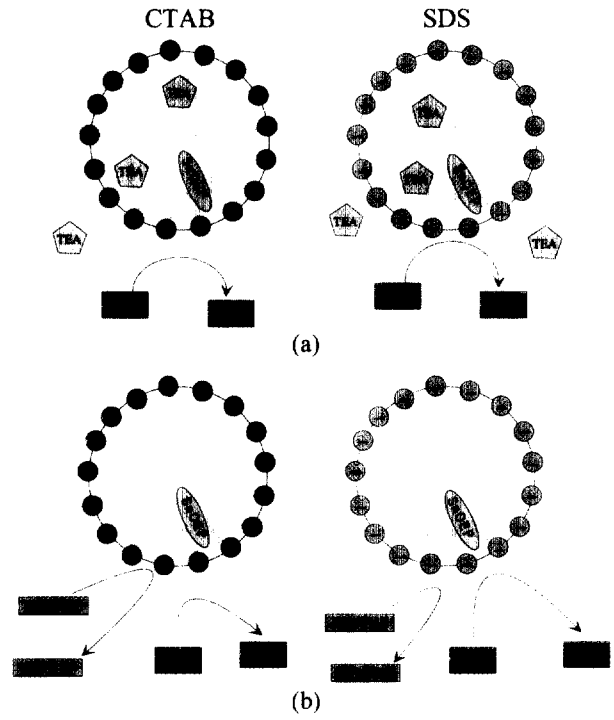

Fig. 8. The photoreactions sensitized by SnOEP in CTAB (left panel) or in SDS (right panel) micelles with TEA (a) or with EDTA (b) as the electron donor.

Table 1
The initial reaction rates of MV^{2+} reduction photosensitized by tin porphyrins in water, micelles[a] and at water/organic solvent interfaces

Porphyrin	Solution type	TEA		EDTA	
		Rate (10^{-7} M^{-1} s^{-1})	Molar rate (s^{-1})	Rate (10^{-7} M^{-1} s^{-1})	Molar rate (s^{-1})
SnLipoP	Hexane/H_2O[b]	2.4 ± 0.3	~0.24	Very small	Very small
	CTAB micelles[c]	0.65 ± 0.1	~0.065	0.41 ± 0.1	~0.041
	SDS micelles[c]	1.8 ± 0.2	~0.18	0.59 ± 0.1	~0.059
SnOEP	Benzene/H_2O[d]	1.1 ± 0.1	0.016 ± 0.02	Very small	Very small
	CTAB micelles[d]	11 ± 1	0.16 ± 0.01	9.6 + 1	0.14 ± 0.01
	SDS micelles[d]	26 ± 3	0.37 ± 0.04	12 + 1	0.17 ± 0.01
SnPP	H_2O (pH 12)[e]	14 ± 1	0.12 ± 0.01	20 + 2	0.17 ± 0.02
	CTAB micelles[e]	22 ± 2	0.19 ± 0.02	21 + 2	0.18 ± 0.02
	SDS micelles[e]	21 ± 2	0.18 ± 0.02	15 + 2	0.13 ± 0.02

Reaction conditions: [a]Micellar concentration = 60 CMC (CTAB CMC = 0.92 mM, SDS CMC = 8.3 mM).
[b]$[MV^{2+}]$ = 0.020 M, [SnLipoP] = ~1 μM, [TEA] = [EDTA] = 0.40 M.
[c]$[MV^{2+}]$ = 0.040 M, [SnLipoP] = ~1 μM, [TEA] = [EDTA] = 0.80 M.
[d]$[MV^{2+}]$ = 0.020 M, [SnOEP] = 7.0 μM, [TEA] = [EDTA] = 0.40 M.
[e]$[MV^{2+}]$ = 0.020 M, [SnPP] = 11.8 μM, [TEA] = [EDTA] = 0.40 M.

similar to that obtained by incorporation of SnOEP into micelles.

The initial rates for SnOEP in micelles are 10–25 times faster than in the two-phase system because of a residence-time enhancement mechanism. For SnOEP, the rate is enhanced in the micellar system because SnOEP anion does not have to diffuse to the water interface, i.e., the porphyrin interfacial residence time and access to the acceptor is enhanced [21–25]. Also, notice that no enhancement is observed for SnLipoP when comparing the two-phase system with the micellar systems. This is because the residence-time enhancement is already present for SnLipoP in the two-phase system. For SnPP, a smaller micellar enhancement is observed in comparing the aqueous (0.12 s^{-1}) and micellar (0.18 and 0.19 s^{-1}) rates.

Another special structural feature of the lipoporphyrin is its highly nonplanar structure caused by the steric constraints of the 12 bulky peripheral substituents. The nonplanarity and presence of bulky substituents of LipoP effectively prevent any porphyrin aggregation [35,36]. In contrast, planar porphyrins like protoporphyrin typically form strong π–π aggregates in aqueous environments [35,56]. Although planar Sn porphyrins generally do not strongly associate because of the strongly bound axial ligands, some Sn porphyrins do weakly associate [57,58].

For SnPP, aggregation in aqueous solution is highly pH-dependent [35]. In Fig. 9, the pH dependence of the UV–visible absorption spectra of SnPP in CTAB micelles (A), in water (B) and in SDS micelles (C) are shown. At high pH in water (B), the Soret band is narrow indicating that the porphyrin is not aggregated. As the pH decreases, the Soret band becomes weaker, and at pH 6, a broad blue-shifted Soret peak appears. A tail also appears at the long-wavelength side of the weakened Soret band, extending out to 500 nm. The red tail probably indicates exciton coupling resulting from some type of aggregation [59]. This pH transition could also be associated with protonation of at least one hydroxide axial ligand. The weakly bound water molecule apparently does not block aggregation. Further decreases in pH result in the gradual disappearance of the blue-shifted peak and greater intensity of the long-wavelength tail as aggregation increases. Thus, for SnPP, the axial ligands do not completely block aggregation, while the nonplanar structure of SnLipoP effectively eliminates aggregation.

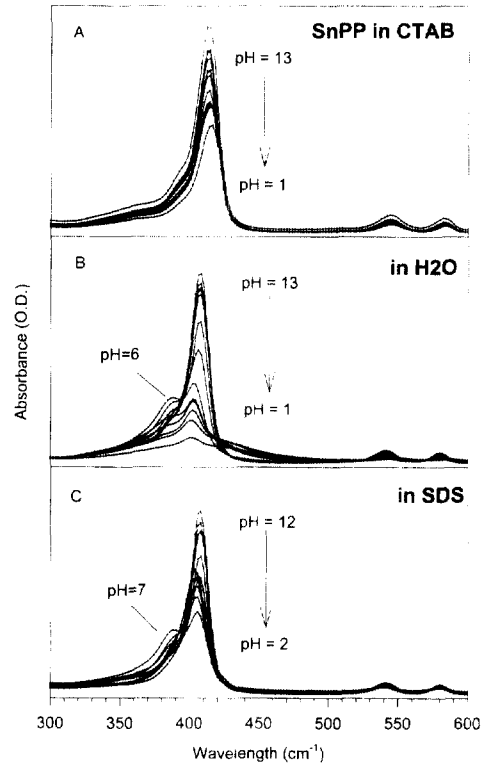

Fig. 9. pH-dependent UV–visible absorption spectra of SnPP in CTAB micelles (A), in water (B), or in SDS micelles (C). The pH was adjusted in intervals 1 pH unit by adding HCl.

In the micellar systems, the macrocycle of SnPP is in a non-aggregating hydrophobic environment as indicated by the absence of a long-wavelength red tail in the absorption spectra in Fig. 9A and C. The absorption data also suggest that the depth of macrocycle insertion into the micellar interior is influenced by the structure of the porphyrin and the charge of the surfactant. The absorption peak near 385 nm for SnPP in SDS micelles is associated with a change in axial ligation. This peak is strongest at pH 7, indicating that a hydroxide ion of SnPP is sensitive to pH and therefore accessible to water. In contrast, for SnPP in CTAB micelles, this peak is absent in the pH range, indicating that the central metal ion is inaccessible to water. These results suggest that the macrocycle of SnPP is entirely located in the hydrophobic environment in CTAB micelles, whereas in SDS micelles, less of the macrocycle is in the hydrophobic environment. These differences in the location of the porphyrin in the micelle are illustrated in Fig. 10 and can be understood in terms of the charge of the micelle. The positively charged head groups of CTAB attract the negatively charged carboxylates of SnPP to the surface of the micelle, leaving the macrocycle in the hydrophobic interior. On the other hand, the negatively charged head group of SDS repels the carboxylates of SnPP, forcing the carboxylates further out of the micellar surface, leading to greater exposure to the aqueous environment. However, in the SDS micelles, there is no evidence of aggregation of SnPP, as occurs in aqueous solution.

3.3. Effect of the electron–donor solubility on photoreaction rates

The difference in the structure makes the porphyrins occupy different positions with respect to the components of the photochemical systems. Further, since the donors, EDTA and TEA, have different solubilities, their access to the photosensitizer molecules differs. For example, for SnPP in water, the initial photoreaction rate with TEA is slower than with EDTA. However, for all three Sn porphyrins, TEA gives a faster rate than EDTA for the water/organic solvent two-phase systems (Table 1).

The differences in rates for the two donors can be understood in terms of the donor distributions in the phases of the ternary reaction mixtures predicted by their relative solubilities in organic and aqueous media. For the aqueous solution, both donor and acceptor molecules have free access to the photosensitizer (SnPP). The photoreaction with TEA is intrinsically slightly slower than with EDTA possibly because TEA is neutral, while EDTA is negatively charged like SnPP.

The two donors distribute differently between hydrophilic and hydrophobic environments in the two-phase reaction systems. This is best illustrated by the water/hexane two-phase reaction for SnLipoP illustrated in Fig. 11. Water-insoluble SnLipoP is in the hexane phase and methylviologen is in the aqueous phase. TEA is soluble in both phases, most importantly, TEA is with the photosensitizer in hexane, and thus

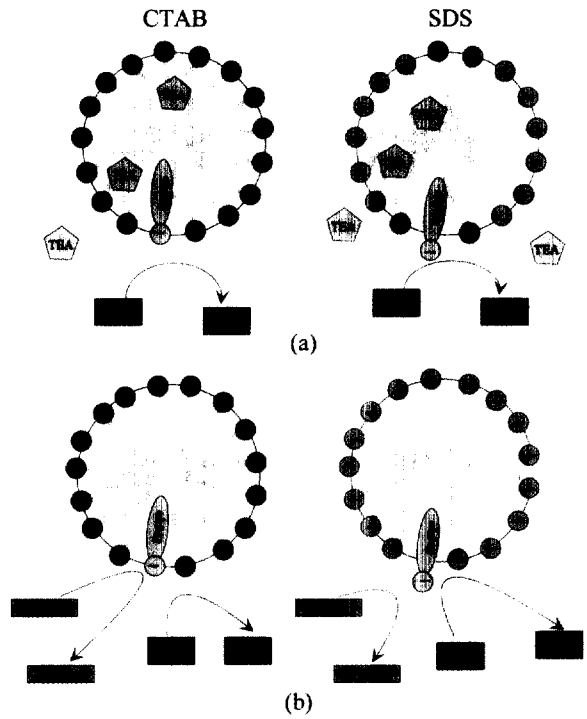

Fig. 10. The photoreactions sensitized by SnPP in CTAB (left panel) or in SDS (right panel) micelles with TEA (a) or with EDTA (b) as the electron donor.

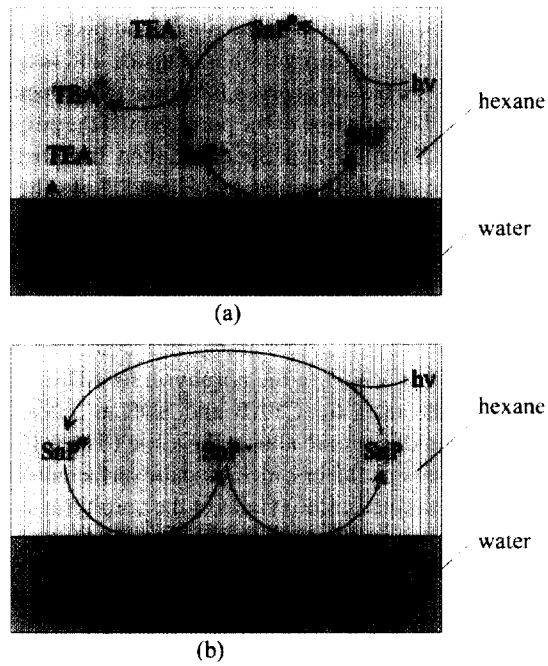

Fig. 11. The photoreactions sensitized by SnLipoP at the hexane/water interface with TEA (a) or with EDTA (b) as the electron donor.

excitation and reduction of the porphyrin are fast. The rate-determining slow step (3) is at the interface, where the porphyrin anion in hexane must deliver the electron across the interface to methylviologen in water. In contrast, EDTA is not soluble in hexane; thus, it must deliver an electron across the interface to excited SnLipoP. Therefore, reduction of

SnLipoP and MV^{2+} is both slow because they must occur across the interface, resulting in a much lower overall rate (Table 1). The same phenomena also occur at the water/benzene interface for SnOEP. Finally, donor solubility is more important for reactions at water/organic solvent interfaces than for micellar solutions, because the small size of the micelles insures greater access of the donor and acceptor to the excited porphyrin and porphyrin anion.

3.4. Micellar effects on reaction rates

Studies on the effects of micelles on reactions photosensitized by porphyrins [21–25] have shown that micelles can promote the photoproduction of $MV^{\bullet+}$ by preventing the formation of a porphyrin–methylviologen complex, and by providing a barrier to back electron transfer. The region of the micellar solution occupied by the donor also affects the photoreaction rate. In particular, since TEA is soluble in both hydrophilic and hydrophobic phases, it reacts with the Sn porphyrin in the micelle more rapidly (Table 1) than EDTA, which cannot penetrate the hydrophobic interior. Our results show some support for these mechanisms in the enhanced rates for SnPP in micellar solutions when TEA is the donor (Table 1). In addition, different initial rates for CTAB and SDS micelles are observed under the same solution conditions. The rate differences in Table 1 can be explained by combining the effect of surfactant charges with the differences in charge and location of the donor and porphyrin.

TEA is neutral and distributes both outside and inside the micelles. Thus, surfactant charges influence the reduction of MV^{2+}, but not the reduction of the porphyrin. If the porphyrin is uncharged (SnLipoP and SnOEP), then the positively charged surface (CTAB) repels MV^{2+} and slows the reaction with the porphyrin. In contrast, a negatively charged surface (SDS) attracts MV^{2+} and accelerates the reaction. Consequently, the photoreactions sensitized by SnLipoP and SnOEP are faster in SDS micelles than in CTAB micelles. These conditions are illustrated in Fig. 7a and8a, showing the closer approach of MV^{2+} to the porphyrin for SDS.

For SnPP, the rates for CTAB and SDS micelles (with TEA as electron donor) are almost the same (Table 1). This results from opposing factors, including the surfactant charge, the negatively charged carboxylates of the porphyrin, and the relative positions of the porphyrin in CTAB and SDS micelles. As discussed earlier, the SnPP reaction is promoted in both CTAB and SDS micelles. However, the reaction is promoted less for SDS than for CTAB because SnPP is more exposed in SDS than in CTAB (see Fig. 10a), possibly allowing unproductive methylviologen–SnPP complex to form. The location of the porphyrin in the micelles differs due to electrostatic interaction between the surfactant charges and the carboxylates of the porphyrin.

EDTA is anionic and is only soluble in the water outside of the micelles. A negatively charged micellar surface prevents EDTA from approaching the porphyrin and slows the formation of porphyrin anion. A positively charged surface attracts EDTA to the surface, speeding up reduction of the porphyrin. Since the charges of EDTA and methylviologen are opposite, the charged surface of a micelle will influence the reaction rates of step (2) and step (3) in opposite ways (as illustrated in Fig. 7b, 8b and 10b). Thus, for SnLipoP or SnOEP, the observed initial reaction rates are not much different in CTAB and SDS micelles (Table 1). For SnPP, the observed rate is considerably slower in SDS than in CTAB micelles due to the different locations of the porphyrin.

4. Summary and conclusions

The photoreactions of EDTA/TEA, porphyrin, and methylviologen at a water–organic solvent interface have a different kinetic behavior from that in homogeneous aqueous and micellar solutions. In general, the photoreaction rates are influenced by the structural properties of porphyrins, the charge and solubility of the electron donors, and the micellar environments. The tin lipoporphyrin shows novel rate-enhancement behavior in the aqueous/organic solvent two-phase system. This is rationalized in terms of the amphiphilic properties of SnLipoP, which results in long residence times at the water–organic solvent interface. In addition, evidence of micellar enhancement of reaction rates by prevention of porphyrin–methylviologen complex, and suppression of back electron transfer are found for all porphyrins investigated. Furthermore, this enhancement is influenced by porphyrin structure-dependent exposure to the aqueous environment and the micellar surface charge.

References

[1] H. Kalyanasundaram, J. Kiwi, M. Grätzel, Helv. Chim. Acta 61 (1978) 2720.
[2] H. Kalyanasundaram, M. Grätzel, Angew. Chem., Int. Ed. Engl. 18 (1979) 701.
[3] H. Kalyanasundaram, M. Grätzel, Helv. Chim. Acta 63 (1980) 478.
[4] I. Okura, N.K. Thuan, J. Mol. Catal. 6 (1979) 227.
[5] I. Okura, N.K. Thuan, J. Chem. Soc., Faraday Trans. 78 (1980) 2209.
[6] A. Harriman, G. Porter, M.C. Richoux, J. Chem. Soc., Faraday Trans. 2 (77) (1981) 833.
[7] A. Harriman, M.C. Richoux, J. Photochem. 15 (1981) 335.
[8] N. Carnieri, A. Harriman, J. Photochem. 15 (1981) 341.
[9] M. Rougee, T. Ebbesen, L. Ghetti, R.V. Bensasson, J. Phys. Chem. 86 (1982) 4404.
[10] M.P. Pileni, Chem. Phys. Lett. 75 (1980) 540.
[11] W. Krüger, J.H. Führhop, Angew. Chem. 94 (1982) 132.
[12] J.A. Mercer-Smith, D. Manzerall, Photochem. Photobiol. 34 (1981) 407.
[13] J.A. Shelnutt, J. Am. Chem. Soc. 105 (1983) 7179.
[14] J.-H. Fuhrhop, W. Krüger, H.H. David, Liebigs Ann. Chem. (1983) 204.
[15] I. Okura, T. Kita, S. Aono, N. Kaji, J. Mol. Catal. 32 (1985) 361.
[16] H. Inoue, K. Chandrasekaran, D.G. Whitten, J. Photochem. 30 (1985) 269.
[17] N.M. Guindy, F.M. Elzawawy, D.Y. Sabry, Collect. Czech. Chem. Commun. 57 (1992) 26.
[18] P.J.G. Coutinho, S.M.B. Costa, J. Photochem. Photobiol. A: Chem. 82 (1994) 149.

[19] G.Z. Wu, M. Hu, H.K. Leung, J. Photochem. Photobiol. A: Chem. 62 (1991) 141.
[20] A. Harriman, G. Porter, N. Searle, J. Chem. Soc., Faraday Trans. 2 76 (1979) 1515.
[21] M.P. Pileni, M. Grätzel, J. Phys. Chem. 84 (1980) 1822.
[22] M.P. Pileni, B. Lerebours, P. Brochette, Y. Chevalier, J. Photochem. 28 (1985) 273.
[23] P. Brochette, M.P. Pileni, Nouv. J. Chim. 9 (1985) 551.
[24] P. Brochette, T. Zemb, P. Mathis, M.P. Pileni, J. Phys. Chem. 91 (1987) 1444.
[25] S.M.B. Costa, J.M.F. Lopes, M.J.T. Martins, J. Chem. Soc. Faraday Trans. 2 (82) (1986) 2371.
[26] M.P. Pileni, Chem. Phys. Lett. 71 (1980) 317.
[27] J.K. Hurst, L.Y.C. Lee, M. Grätzel, J. Chem. Soc. 105 (1983) 7048.
[28] J. Kiwi, M.J. Grätzel, J. Am. Chem. Soc. 100 (1978) 6314
[29] J. Kiwi, M.J. Grätzel, J. Phys. Chem. 84 (1980) 1503.
[30] C.A. Jones, L.E. Weaner, R.A. Mackay, J. Phys. Chem. 84 (1980) 1495.
[31] C.K. Grätzel, M. Grätzel, J. Phys. Chem. 86 (1982) 2710.
[32] D. Mandler, Y. Degani, I.J. Willner, J. Phys. Chem. 88 (1984) 4366.
[33] U. Resch, S.M. Hubig, M.A. Fox, Langmuir 7 (1991) 292.
[34] A. Ulman, An Introduction to Ultrathin Organic Films from Langmuir–Blodgett to Self-Assembly, Academic Press, 1991, p. 396.
[35] X. Song, M. Miura, X. Xu, K.K. Taylor, S.A. Majumder, J.D. Hobbs, J. Cesarano, J.A. Shelnutt, Langmuir 12 (1996) 2019.
[36] M. Miura, S.A. Majumder, J.D. Hobbs, M.W. Renner, L.R. Furenlid, J.A. Shelnutt, Inorg. Chem. 33 (1994) 6078.
[37] J.A. Shelnutt, X.-Z. Song, J.-G. Ma, S.-L. Jia, W. Jentzen, C.J. Medforth, Chem. Soc. Rev. 27 (1998) 31.
[38] S.L. Mayo, B.D. Olafson, W.A. Goddard III, J. Phys. Chem. 94 (1990) 8897.
[39] J.A. Shelnutt, C.J. Medforth, M.D. Berber, K.M. Barkigia, K.M. Smith, J. Am. Chem. Soc. 113 (1991) 4077.
[40] M. Abe, T. Kitagawa, Y. Kyogoku, J. Chem. Phys. 69 (1978) 4526.
[41] T. Kitagawa, M. Abe, H. Ogoshi, J. Chem. Phys. 69 (1978) 4516.
[42] X.Y. Li, R.S. Czernuszewicz, J.R. Kincaid, T.G. Spiro, J. Am. Chem. Soc. 111 (1989) 7012.
[43] X.Y. Li, R.S. Czernuszewicz, J.R. Kincaid, P. Stein, T.G. Spiro, J. Phys. Chem. 94 (1990) 47.
[44] T.D. Brennan, W.R. Scheidt, J.A. Schelnutt, J. Am. Chem. Soc. 110 (1988) 3919.
[45] W. Jentzen, M.C. Simpson, J.D. Hobbs, X.Z. Song, T. Ema, N.Y. Nelson, C.J. Medforth, K.M. Smith, M. Veyrat, M. Mazzanti, R. Ramasseul, J.C. Marchon, T. Takeuchi, W.A. Goddard III, J.A. Shelnutt III, J. Am. Chem. Soc. 117 (1995) 11085.
[46] J.D. Hobbs, S.A. Majumder, L. Luo, G.A. Sickelsmith, J.M.E. Quirke, C.J. Medforth, K.M. Smith, J.A. Shelnutt, J. Am. Chem. Soc. 116 (1994) 3261.
[47] L.D. Sparks, J.R. Chamberlain, P. Hsu, M.R. Ondias, B.A. Swanson, P.R. Ortiz de Montellano, J.A. Shelnutt, Inorg. Chem. 32 (1993) 3153.
[48] L.D. Sparks, W.R. Scheidt, J.A. Shelnutt, Inorg. Chem. 31 (1992) 2191.
[49] C.J. Medforth, M.O. Senge, T.P. Forsyth, J.D. Hobbs, J.A. Shelnutt, K.M. Smith, Inorg. Chem. 33 (1994) 3865.
[50] L.D. Sparks, C.J. Medforth, M.S. Park, J.R. Chamberlain, M.R. Ondrias, M.O. Senge, K.M. Smith, J.A. Shelnutt, J. Am. Chem. Soc. 115 (1993) 581.
[51] X.Z. Song, W. Jentzen, S.L. Jia, L. Jaquinod, D.J. Nurco, C.J. Medforth, K.M. Smith, J.A. Shelnutt, J. Am. Chem. Soc. 118 (1996) 12975.
[52] J.A. Shelnutt, US Patent 4,568,435, 1986.
[53] D.G. Whitten, Acc. Chem. Res. 13 (1980) 83.
[54] J.H. Furhop, K.M. Kadish, D.G. Davis, J. Am. Chem. Soc. 95 (1973) 5140.
[55] M. Gouterman, F.P. Schwarz, P.D. Smith, J. Chem. Phys. 59 (1973) 676.
[56] R.G. Alden, M.R. Ondrias, J.A. Shelnutt, J. Am. Chem. Soc. 112 (1990) 691.
[57] J.A. Shelnutt, M.M. Dobry, J.D. Satterlee, J. Phys. Chem. 88 (1984) 4980.
[58] J.A. Shelnutt, J. Phys. Chem. 88 (1984) 6121.
[59] M. Gouterman, D. Holten, E. Lieberman, Chem. Phys. 25 (1977) 139.